



## Application of Periwinkle Shell Ash as Photocatalyst in the Heterogeneous Photocatalytic Degradation of Aniline in Aqueous Solution

F.A. Aisien<sup>1</sup>, N.A. Amenaghawon<sup>1</sup>, F.O. Oshomogho<sup>1</sup>

<sup>1</sup>Department of Chemical Engineering, University of Benin, Benin City, Edo State, Nigeria.

Received 14 July 2014; Revised 4 September 2014; Accepted 21 September 2014.

\*Corresponding Author. E-mail: [andrew.amenaghawon@uniben.edu](mailto:andrew.amenaghawon@uniben.edu); Tel: (+2348069275563)

### Abstract

Periwinkle shell ash (PSA) was used as a photocatalyst in the photocatalytic degradation of aniline in aqueous solution. The effects of contact time, initial aniline concentration, PSA dosage, pH and hydrogen peroxide (H<sub>2</sub>O<sub>2</sub>) on the process were investigated. The results show that maximum photocatalytic degradation efficiency was obtained at a contact time of 100 minutes, initial aniline concentration of 50 mg/L, PSA dosage of 2 g/L and pH of 8. The addition of H<sub>2</sub>O<sub>2</sub> improved the photocatalytic degradation efficiency to almost 100 percent. The adsorption equilibrium was well described by the Langmuir isotherm equation ( $R^2=0.951$ ). The kinetics of the process was well described by the pseudo first order and Langmuir-Hinshelwood kinetic models while the diffusion mechanism was modelled by the intra particle diffusion model ( $R^2>0.90$ ).

**Keywords:** Periwinkle shell ash, Aniline, Adsorption, Kinetics, Isotherm, Equilibrium

### Introduction

Aniline is one of the most widely used substances in the chemical industry. It finds application as a raw material in the production of isocyanate, dyes, synthetic rubber, polymers, herbicides, pesticides, fungicides and pharmaceuticals [1]. It is released into the environment through effluents from these processes. Aniline has been reported to be toxic and harmful to both humans and animals and the degree of toxicity is dependent on the amount and time of exposure [2]. As a result of the toxicity and recalcitrance of aniline, a lot of attention has been focused on removing it from the environment in an effective and economical manner [3].

Several methods have been utilised for the treatment of aniline contaminated effluents. These methods include adsorption [4], chemical oxidation [5], biological [6] and catalytic wet air oxidation [7]. However, the major limitation of these methods has to do with the disposal of the sludge generated in the course of treatment, low efficiency and reaction rates as well applicability within a narrow range pH range [8]. Among chemical methods, photocatalysis has emerged as a promising technique for the degradation of organic pollutants in aqueous media. It is based on the surface activation of semiconductors notably zinc oxide (ZnO) and titanium dioxide (TiO<sub>2</sub>) by ultraviolet (UV) radiation. The most significant advantage of this technique is that it can be used to degrade most organic compounds which are not amenable to other conventional treatment processes. It is faster than most bioprocesses and cheaper than ozonolysis and radiation based processes as it can be carried out under direct sunlight, making it able to operate independent of any external power source [9]. Being one of the most common photocatalyst, TiO<sub>2</sub> possesses a lot of positive attributes such as low cost, high photocatalytic activity and nontoxicity [10,11]. Nevertheless, TiO<sub>2</sub> has certain important deficiencies as its response and capacity to utilise radiation is limited in the UV region. Thus it requires a high power UV excitation source [2,12]. In addition, the capacity for catalyst recovery is also limited. Therefore it is important to explore alternative photocatalysts with better recovery and light absorption capacity, with important focus on locally sourced catalysts such as periwinkle shell ash.

Periwinkle shell is waste product generated from the consumption of periwinkle, a small greenish-blue marine snail found in many coastal communities in Nigeria. The shells are typically disposed of after consuming the edible part as sea food thereby constituting an environmental burden. Though some of these shells are utilised for the local manufacture of break pads, as coarse aggregate in concrete and filling of water logged areas, a

significant quantity of these shells are still disposed of annually. The reuse capacity of these shells can be expanded by utilising them for the development of value added products such as photocatalysts.

The aim of this study is to investigate the potential use of periwinkle shell ash as photocatalyst for the photocatalytic degradation of aniline in aqueous solution. The effects of factors such as contact time, initial aniline concentration, catalyst dosage, pH and hydrogen peroxide (H<sub>2</sub>O<sub>2</sub>) on the degradation process were investigated. The photocatalytic degradation of aniline was further evaluated by carrying out kinetic and isotherm studies.

## 2. Materials and methods

### 2.1. Preparation and characterisation of photocatalyst (Periwinkle shell ash)

Periwinkle shells were obtained from Warri in Delta State of Nigeria. The shells were washed and dried in an oven at 110°C to constant mass, followed by crushing and calcination at 600°C in a muffle furnace and subsequent sieving to obtain fine particles (< 350µm) of periwinkle shell ash (PSA). The calcination was carried out in such a way that neither the fuel for heating nor the exhaust gases came in contact with the material that was being calcined. The prepared PSA was characterised by determining the composition using X-Ray Fluorescence (XRF) analysis [13]. The surface structure and other properties of the PSA were evaluated by nitrogen adsorption method at -196°C [14]. The surface area of the PSA was determined using the standard BET equation [15]. The bulk density of the PSA was determined following standard methods [16].

### 2.2. Preparation of aniline solution

Analytical reagent grade aniline, provided by Griffin and George Ltd, Loughborough, England was used in this study. A stock solution of aniline was prepared by dissolving an appropriate amount of aniline in 1000 mL of deionised water. Working solutions with different concentrations of aniline were prepared by appropriate dilutions of the stock solution with deionised water immediately prior to their use.

### 2.3. Photocatalytic degradation studies

Batch photocatalytic degradation of aniline using PSA in the presence of UV radiation from sunlight was carried out in mechanically agitated 250 mL jacketed glass flasks with a working volume of 100 mL. The sunlight was directed to the reaction vessel using a converging lens with a focal length of 14 cm. The sunlight experiments were carried out between 9:00 A.M and 2:30 P.M. on a sunny day. The light intensity was measured using UV light intensity detector (Lutron UV-340), and was found to be in the range of 0.370 to 0.480 mW/cm<sup>2</sup>. For each experimental run, the appropriate amount of PSA was added to the aqueous solution of aniline of the desired concentration and the suspension was magnetically stirred without any permanent air bubbling [17]. The temperature was maintained at 25 °C and monitored throughout the process [9]. The effect of contact time, initial aniline concentration, PSA dosage, H<sub>2</sub>O<sub>2</sub> and pH of solution on the degradation efficiency was investigated. At the end of each experiment the agitated solution mixture was filtered through a 0.45 µm membrane and the residual concentration of aniline was determined spectrophotometrically at a wavelength of 248 nm. The percentage photocatalytic degradation of aniline was calculated using the equation:

$$\% \text{ Photodegradation} = \frac{C_o - C_t}{C_o} \times 100 \quad (1)$$

where  $C_o$  and  $C_t$  are the initial and the instantaneous concentration of aniline respectively.

## 3. Results and discussion

### 3.1. Characterisation of periwinkle shell ash

The results of X-Ray Fluorescence (XRF) analysis for determining the chemical composition of PSA is presented in Table 1. The major constituents of the PSA used in this study were calcium oxide (CaO) and silicon dioxide (SiO<sub>2</sub>) which respectively accounted for 41.3 and 33.2% of the weight of PSA. Some other oxides such as K<sub>2</sub>O, Na<sub>2</sub>O, TiO<sub>2</sub> and MnO<sub>2</sub> were also found to be present in small amounts. Some of the oxides presented in Table 1 have been reported to possess photocatalytic properties thus supporting the choice of PSA for this study [18,19]. The surface area, bulk density and porosity of the PSA used in this study are presented in Table 2. Results similar to those presented in Tables 1 and 2 have been reported by other researchers [20,21].

**Table 1:** Chemical composition of PSA

Chemical Component	Composition (wt %)
MgO	1.2
SiO <sub>2</sub>	33.2
ZnO	3.2
Fe <sub>2</sub> O <sub>3</sub>	5.0
MnO <sub>2</sub>	1.0
Al <sub>2</sub> O <sub>3</sub>	9.2
CaO	41.3
CuO	1.3
K <sub>2</sub> O	1.4
Na <sub>2</sub> O	1.38
TiO <sub>2</sub>	0.02
Loss on Ignition	1.8

**Table 2:** Physical properties of PSA

Property	Value
Surface area (m <sup>2</sup> /g)	400
Bulk density (kg/m <sup>3</sup> )	2940
Porosity (-)	0.004

### 3.2. Effect of contact time

The effect of contact time on the photocatalytic degradation of aniline is shown in Figure 1. Photocatalytic degradation of aniline was rapid during the first 40 minutes of the process indicating a fast kinetic process. This observation could be attributed to the abundant active sites available on the photocatalyst surface. The rate of the photocatalytic degradation reaction was observed to slow down in the latter stages of the reaction as seen from the almost constant trend in the photocatalytic degradation efficiency. This could be as a result of the limited number of active sites on the catalyst surface as the sites are then occupied by the aniline molecules [22]. The constant trend observed at the later stages of the process could also be attributed to the system reaching equilibrium which means that there was no significant change in the rate of photocatalytic degradation.

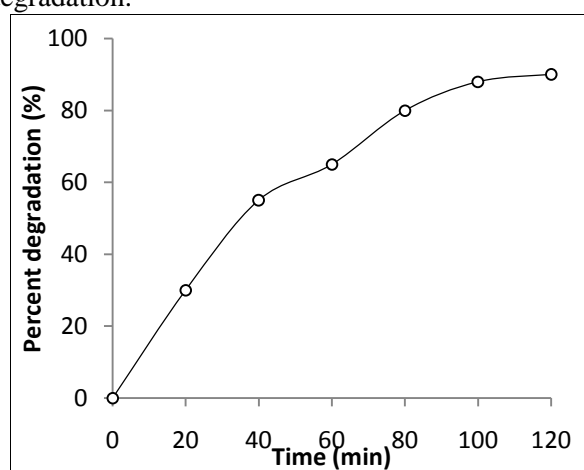


**Figure 1:** Effect of contact time on the photocatalytic degradation of aniline (pH 8; PSA dose, 2 g/L; initial concentration, 50 mg/L; temperature, 25 °C)

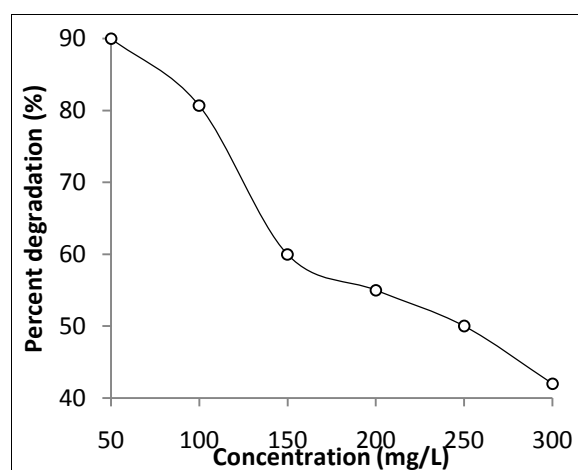


**Figure 2:** Effect of concentration on the photocatalytic degradation of aniline (pH 8; PSA dose, 2 g/L; temperature, 25 °C)

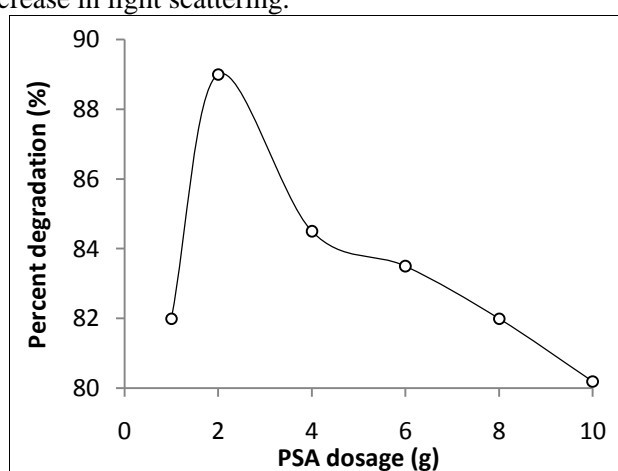
### 3.3. Effect of initial aniline concentration

Figure 2 shows the effect of initial concentration of aniline on the photocatalytic degradation process. For the concentration 50 mg/L, about 90% degradation was recorded after about 100 minutes, but for the higher concentrations such as 150 to 300 g/L, the photocatalytic process proceeded with lower efficiency. The lower

efficiencies recorded at high concentrations of aniline could be as a result of the formation of several layers of adsorbed aniline molecules on the photocatalyst surface. This inhibits the reaction of the aniline molecules with the holes or hydroxyl and oxygen free radicals ( $\bullet\text{OH}$  and  $\text{O}_2^{\bullet-}$ ) as the aniline molecules have limited access to these radicals [23-25].

### 3.4. Effect of photocatalyst dosage

The result of aniline degradation as a function of PSA dosage is shown in Figure 3. The result showed that the degradation efficiency increased to a maximum of about 89% when the PSA dosage was increased from 1 to 2 g/L. Increasing the PSA dosage beyond 2 g/L resulted in a decrease in the degradation efficiency. This observation might be attributed to the so-called shielding effect which occurs after exceeding the optimal catalyst dosage as the suspended PSA particles reduces the penetration of the light in the solution [25,26]. A similar observation was reported by Suri et al. [27] for the degradation of toluene, trichloroethylene and methylethylketone using  $\text{TiO}_2$ . They observed that using a higher dosage of the catalyst might not be advisable as a result of possible aggregation and reduced irradiation field inside the reactor as a result of increase in light scattering.



**Figure 3:** Effect of PSA dosage on the photocatalytic degradation of aniline (pH 8; initial concentration, 50 mg/L; temperature, 25°C)

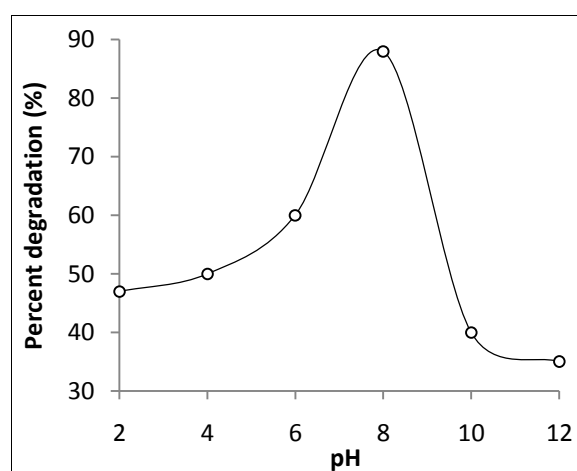


**Figure 4:** Effect of pH on the photocatalytic degradation of aniline (initial concentration, 50 mg/L PSA dose, 2 g/L; temperature, 25°C)

### 3.5. Effect of pH

Figure 4 shows the effect of pH on the degradation process. The result shows that the process was strongly dependent on the pH of the solution. This could be attributed to the amphoteric behaviour of most of the semiconductor oxides present in PSA [24]. The degradation efficiency increased from 47 to 88% when the pH was increased from 2 to 8. Further increase in pH did not impact positively on the degradation process. Abdollahi et al. [23] reported similar observations for the photocatalytic degradation of *m*-cresol by Zinc Oxide under visible light irradiation. The initial increase in photocatalytic degradation with increase in pH might have resulted from the decrease in the electrostatic repulsive forces and subsequently increased interaction between the aniline molecules and the photocatalyst surface [28]. The decrease in photocatalytic degradation efficiency observed beyond the optimum pH might have resulted from the excess of negatively charged hydroxyl ions which makes the surface of the photocatalyst to be negatively charged. The negatively charged photocatalyst surface thus repels the approaching negatively charged aniline molecules with a consequent reduction in the photocatalytic degradation efficiency [29].

### 3.6. Effect of hydrogen peroxide ( $\text{H}_2\text{O}_2$ )

Figure 5 shows the effect of  $\text{H}_2\text{O}_2$  on the photocatalytic degradation process. The degradation efficiency increased with increase in  $\text{H}_2\text{O}_2$  loading with almost 100% degradation achieved when 10  $\text{cm}^3$  of hydrogen peroxide per litre of solution was used.  $\text{H}_2\text{O}_2$  is a strong electron acceptor and has been reported to generate hydroxyl radicals in solution. The free radicals generated by  $\text{H}_2\text{O}_2$  in solution create a strong oxidation environment which favours the photocatalytic degradation process [25].

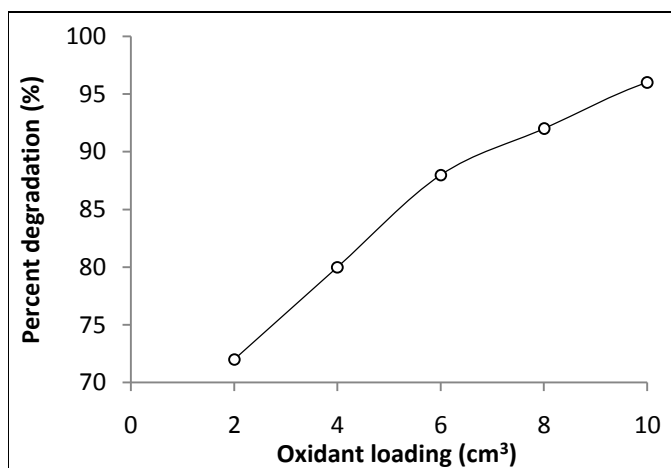


**Figure 5:** Effect of H<sub>2</sub>O<sub>2</sub> loading on the photocatalytic degradation of aniline (pH, 8; initial concentration, 50 mg/L PSA dose, 2 g/L; temperature, 25°C)

### 3.7. Kinetic modelling

The kinetics of the photocatalytic degradation process was studied using three kinetic models namely pseudo first-order, intra particle diffusion and Langmuir-Hinshelwood kinetic models.

#### 3.7.1 Pseudo first order model

The pseudo first-order equation is expressed as follows:

$$r = -\frac{dC}{dt} = kC \quad (2)$$

The pseudo first order reaction rate constant,  $k$  was obtained from the integrated linear form of Equation (2) as follows:

$$k = \frac{\ln C_o / C_i}{t} \quad (3)$$

The plot of  $\ln C_o / C_i$  versus  $t$  resulted in a linear relationship from which the value of  $k$  was determined as shown in Figure 6. The pseudo first order rate constants calculated from the plot at different initial aniline concentrations are given in Table 3. The straight line plots obtained for the range of aniline concentration investigated show that the pseudo first order equation was applicable for the range of aniline concentration.

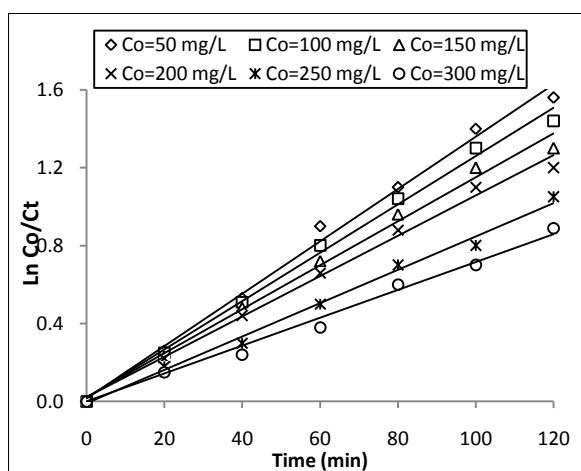


**Figure 6:** Pseudo first order model fitted to batch data for aniline photocatalytic degradation by PSA (pH, 8; PSA dose, 2 g/L; temperature, 25 °C)

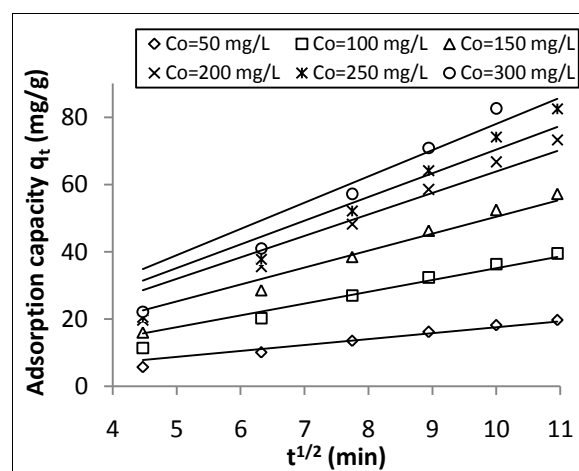


**Figure 7:** Intra particle diffusion model fitted to batch data for aniline photocatalytic degradation by PSA (pH, 8; PSA dose, 2 g/L; temperature, 25 °C)

### 3.7.2 Intra particle diffusion model

The intra particle diffusion model which describes the diffusion mechanism inside the catalyst particle is presented as follows [30]:

$$q_t = K_p t^{1/2} + C \quad (4)$$

$K_p$  is the intra particle diffusion rate constant ( $\text{mg g}^{-1} \text{ min}^{-1/2}$ ) and  $C$  is a measure of boundary layer effect. Figure 7 shows the plot of  $q_t$  versus  $t^{1/2}$  from which the values of  $K_p$  and  $C$  were calculated and the results are presented in Table 3. The values of  $C$  were obtained as zero for the range of aniline concentration indicating that there was no boundary layer effect. The high  $R^2$  values obtained for the kinetic parameters estimated within the concentration range investigated show that the intra particle diffusion model was able to describe the diffusion mechanism of the photocatalytic degradation process.

**Table 3:** Kinetic constant parameter values for the photocatalytic degradation of aniline

$C_o$ (mg/L)	Pseudo first order		Intra-particle diffusion			Langmuir-Hinshelwood		
	$k$	$R^2$	$K_p$	$C$	$R^2$	$k_r$	$K$	$R^2$
50	0.0134	0.993	1.756	0.00	0.954	4.66	0.0036	0.991
100	0.0128	0.998	3.511	0.00	0.954			
150	0.0113	0.993	5.037	0.00	0.941			
200	0.0104	0.994	6.384	0.00	0.939			
250	0.0086	0.994	7.056	0.00	0.920			
300	0.0071	0.989	7.800	0.00	0.910			

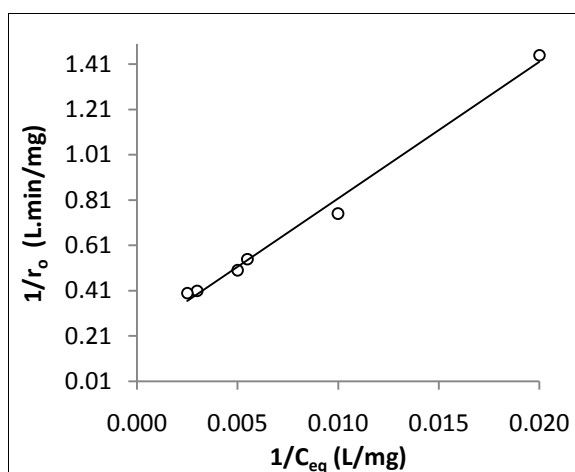


**Figure 8:** Langmuir-Hinshelwood model fitted to batch equilibrium data for aniline photocatalytic degradation by PSA (pH, 8; PSA dose, 2 g/L; temperature, 25 °C)

### 3.7.3 Langmuir-Hinshelwood model

The Langmuir-Hinshelwood kinetic equation developed by Turchi and Ollis, [31] has often been used to model the kinetics of most heterogeneous processes. The equation is expressed as follows:

$$r_o = -\frac{dc}{dt} = \frac{k_r K C_{eq}}{1 + K C_{eq}} \quad (5)$$

$r_o$  is the initial rate of reaction in  $\text{mg/L.min}$ ,  $k_r$  is the rate constant for photocatalysis in  $\text{mg/L min}$ ,  $K$  is the rate constant for adsorption in  $\text{L/mg}$ ,  $C_{eq}$  is the concentration of bulk solution in  $\text{mg/L}$  at adsorption equilibrium,  $c$  is the concentration of bulk solution at any time  $t$ . Equation (5) was linearised as follows:

$$\frac{1}{r_o} = \frac{1}{k_r K C_{eq}} + \frac{1}{k_r} \quad (6)$$

Experimental values of  $1/r_o$  were plotted against  $1/C_{eq}$  as shown in Figure 8 and the values of the calculated constants are presented in Table 3. The high  $R^2$  value obtained shows that the model was also able to describe the kinetics of the process.

### 3.8 Isotherm Studies

The Langmuir and Freundlich adsorption isotherm models were used to describe the equilibrium of the photocatalytic degradation process.

#### 3.8.1 Langmuir isotherm

The linear form of the Langmuir equation is given as [32]:

$$\frac{C_e}{q_e} = \frac{1}{q_o} C_e + \frac{1}{K_L q_o} \quad (7)$$

$q_o$  is the maximum adsorption capacity (mg/g) of the adsorbent while  $K_L$  is the adsorption constant (L/mg). Experimental values of  $C_e/q_e$  were plotted against  $C_e$  as shown in Figure 9 and the plot was used to calculate the values of  $q_o$  and  $K_L$  and the values are shown in Table 4.

**Table 4:** Kinetic parameters for Langmuir and Freundlich isotherms

Langmuir isotherm			Freundlich isotherm		
$q_o$ (mg/g)	$K_L$ (L/mg)	$R^2$	$K_f$ (mg/g)	n	$R^2$
1.453	0.0204	0.951	0.0591	1.623	0.944

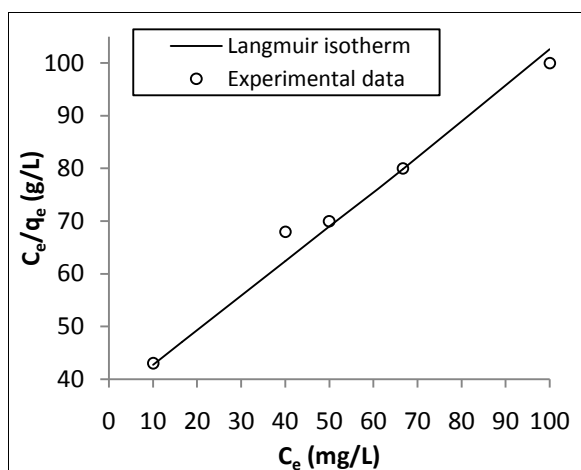


**Figure 9:** Langmuir isotherm model linearised to equilibrium data for aniline photocatalytic degradation by PSA (pH, 8; PSA dose, 2 g/L; temperature, 25 °C)

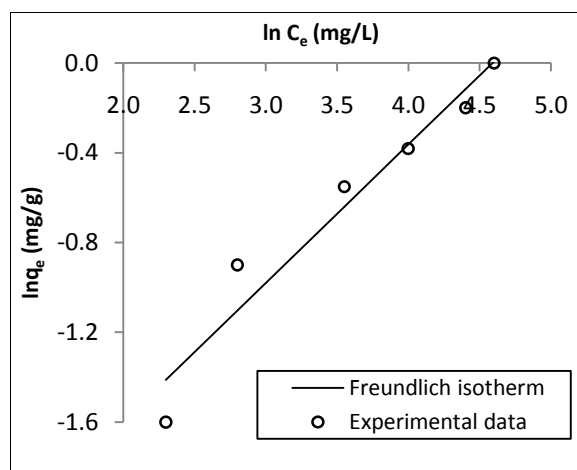


**Figure 10:** Freundlich isotherm model linearised to equilibrium data for aniline photocatalytic degradation by PSA (pH, 8; PSA dose, 2 g/L; temperature, 25 °C)

#### 3.8.2 Freundlich isotherm

The Freundlich isotherm equation is expressed as follows:

$$q_e = K_f (C_e)^{1/n} \quad (8)$$

The equation was linearised to obtain the following:

$$\ln q_e = \ln K_f + 1/n \ln C_e \quad (9)$$

$K_f$  and  $n$  are the Freundlich constants related to the adsorption capacity and adsorption intensity respectively. A linear plot of  $\ln q_e$  against  $\ln C_e$  as shown in Figure 10 was employed to obtain the values of  $K_f$  and  $n$ . The values of these parameters as well as the correlation coefficient ( $R^2$ ) of the Freundlich equation are given in Table 4. The values of  $n$  between 1 and 10 typically indicate a favourable adsorption process. The high values of the correlation coefficients as shown in Table 4 indicate that the data fitted well to both isotherm equations.

## Conclusion

The batch photocatalytic degradation of aniline in aqueous solution using periwinkle shell ash as photocatalyst was investigated. The photocatalytic degradation process was influenced by factors such as contact time, initial aniline concentration, PSA dosage, presence of oxidant (H<sub>2</sub>O<sub>2</sub>) and solution pH. The optimum adsorption condition are as follows: contact time, 100 minutes; initial aniline concentration, 50 mg/L; PSA dosage, 2 g/L; pH, 8. The addition of H<sub>2</sub>O<sub>2</sub> enhanced the photocatalytic degradation process with almost 100 percent degradation achieved. The adsorption equilibrium and diffusion mechanism were well described by the Langmuir isotherm and intra-particle diffusion models while the photocatalytic degradation kinetics was well described by the pseudo first order and Langmuir-Hinshelwood kinetic models with high correlation coefficient values ( $R^2 > 0.90$ ).

## References

1. Mitadera, M., Spataru, N., Fujishima, A. *J. Appl. Electrochem.* 34 (2004) 249.
2. Liu, G., Wang, Z., Zheng, W., Yang, S., Sun, C., *Adv Condensed Matter Phys.* 2014 (2014) 1
3. Li, J., Jin, Z., *J. Hazard. Mater.* 172 (2009) 432.
4. O'Brien, J., O'Dwyer, T.F., Curtin, T., *J. Hazard. Mater.* 159 (2008) 476.
5. Sarasa, J., Cortes, S., Ormad, P., Gracia, R., Ovelleiro, J.L., *Water Res.* 36 (2002) 3035.
6. Goonewardena, N., Nasu, M., Okuda, A., Tani, K., Takubo, Y., Kondo, M., *Biomed. Environ. Sci.* 5 (1992) 25.
7. Ersoaz, G., Atalay, S., *Ind. Eng. Chem. Res.* 50 (2011) 310.
8. Laoufi, N.A., Tassalit, D., Bentahar, F., *Global Nest J.* 10 (2008) 404.
9. Lair, A., Ferronato, C., Chovelon, J.M., Herrmann, J.M., *J. Photochem Photobiol A: Chem.* 193 (2008) 193.
10. Ahmed, S., Rasul, M.G., Martens, W.N., Brown, R., Hashib, M.A., *Water, Air, & Soil Pollut.* 215 (2011) 3.
11. Mirkhani, V., Tangestaninejad, S., Moghadam, M., Habibi, M.H., Vartooni, A.R., *J. Iranian Chem. Soc.* 6 (2009) 800.
12. Chatterjee, D., Dasgupta, S., *J. Photochem Photobiol.* 6 (2005) 186.
13. Aku, S.Y., Yawas, D.S., Madakson, P.B., Amaren, S.G., *Pacific J. Sci. Technol.* 13 (2012) 57.
14. Aisien, F.A., Amenaghawon, N.A., Akhidenor, S.A., *J. Sci. Res. Rep.* 2(2013) 497.
15. Walton, K.S., Snurr, R.Q., *J. Am Chem. Soc.* 129 (2007) 8552.
16. APHA-AWWA-WPCF., *Standard methods for the examination of water and wastewater.* American Public Health Association, New York. (1989)
17. Aisien, F.A., Amenaghawon, N.A. and Ekpenisi, E.F., *J. Eng. Appl. Sci.* 9 (2013) 11.
18. Palmisano, G., Augugliaro, V., Pagliaro, M., Palmisano, L., *Chem. Commun.* 33 (2007) 3425.
19. Sakthivel, S., Neppolian, B., Shankar, M.V., Arabindoo, B., Palanichamy, M., Murugesan, V., *Solar Energy Mater Solar Cells.* 77 (2003) 65.
20. Owabor, C.N., Iyaomolere, A.I., *J. Appl. Sci. Environ. Manage.* 17 (2013) 321.
21. Umoh, A.A., Olusola, K.O., *Int. J. Sustainable Construc Eng Technol.* 3 (2012) 45.
22. Akyol, A., Yatmaz, H.C., Bayramoglu, M., *Appl Catal B: Environ.* 54 (2004) 19.
23. Abdollahi, Y., Abdullah, A.H., Zainal, Z., Yusof, N.A., *Int. J. Chem.* 3 (2011) 31.
24. Behnajady, M.A., Modirshahla, N., Hamzavi, R., *J. Hazard Mater.* 133 (2006) 226
25. Grzechulska, J., Morawski, A.W., *Appl Catal. B: Environ.* 36 (2002) 45.
26. Konstantinou, I.K. and Albanis, T.A., *Appl. Catal B: Environ.* 49 (2004) 1.
27. Suri, R.P.S., Liu, J., Hand, D.W., Crittenden, J.C., Perram, D.L., Mullins, M.E., *Water Environ. Res.* 65 (1993) 665.
28. Kosmulski, M., *J. Colloid Interface Sci.* 298 (2006) 730.
29. Menkiti, M.C., Nnaji, P.C., Onukwuli, O.D., *Nature and Science*, 7 (2009) 1.
30. Weber W.J., Morris, J.C., *J. Sanit Eng Div. Am. Soc. Civil Eng.* 89 (1963) 31.
31. Turchi, C.S., Ollis, D.F., *J. Catal.* 122 (1990) 178.
32. Langmuir, I., *J. Am. Chem. Soc.* 40 (1914) 361.

(2015) ; <http://www.jmaterenvironsci.com>